



**HAL**  
open science

## Joint use of compressible large-eddy simulation and Helmholtz solvers for the analysis of rotating modes in an industrial swirled burner

Laurent Selle, Laurent Benoit, Thierry Poinsot, Franck Nicoud, Werner Krebs

### ► To cite this version:

Laurent Selle, Laurent Benoit, Thierry Poinsot, Franck Nicoud, Werner Krebs. Joint use of compressible large-eddy simulation and Helmholtz solvers for the analysis of rotating modes in an industrial swirled burner. *Combustion and Flame*, 2006, 145 (1-2), pp.194-205. 10.1016/j.combustflame.2005.10.017 . hal-00908256

**HAL Id: hal-00908256**

**<https://hal.science/hal-00908256>**

Submitted on 22 Nov 2013

**HAL** is a multi-disciplinary open access archive for the deposit and dissemination of scientific research documents, whether they are published or not. The documents may come from teaching and research institutions in France or abroad, or from public or private research centers.

L'archive ouverte pluridisciplinaire **HAL**, est destinée au dépôt et à la diffusion de documents scientifiques de niveau recherche, publiés ou non, émanant des établissements d'enseignement et de recherche français ou étrangers, des laboratoires publics ou privés.

# Joint use of Compressible Large-Eddy Simulation and Helmholtz solvers for the analysis of rotating modes in an industrial swirled burner

L. Selle <sup>a</sup>, L. Benoit <sup>a</sup>, T. Poinso <sup>b</sup>, F. Nicoud <sup>c</sup> and W. Krebs <sup>d</sup>

<sup>a</sup>*CERFACS, CFD team, 42 Av. G. Coriolis, 31057 Toulouse Cedex, France*

<sup>b</sup>*IMF Toulouse, UMR CNRS/INP-UPS 5502, Allée du Pr. C. Soula, 31400  
Toulouse CEDEX, France*

<sup>c</sup>*Université Montpellier II UMR CNRS 5149, France*

<sup>d</sup>*Siemens PG, Mullheim, Germany*

---

## Abstract

Rotating modes are instabilities which are commonly observed in swirling flows. This paper shows that, in complex geometry swirled combustors, such modes can appear for both cold and reacting conditions but that they have different sources: while the cold flow rotating mode is essentially hydrodynamic and corresponds to the well-known PVC (Precessing Vortex Core) observed in many swirled unconfined flows, the rotating structure observed for the reacting case inside the combustion chamber is not hydrodynamically but acoustically controlled. The two transverse acoustic modes of the combustion chamber couple and create a rotating motion of the flame which leads to a self-sustained turning mode which has the features of a classical PVC but a very different source (acoustics and not hydrodynamics). These

results are obtained using two complementary tools: compressible LES (Large Eddy Simulations) which solve the turbulent flow and the acoustics simultaneously (but at a high cost) and Helmholtz solvers which freeze the flow and extract only the acoustic modes using linear acoustics assumptions.

*Key words:* Large-Eddy Simulation, Acoustics, Helmholtz solver, complex geometry.

---

## 1 Introduction

Large-Eddy Simulation (LES) methodologies constitute intermediate steps between steady state calculations (RANS) and Direct Numerical Simulation (DNS) [1]. During the past ten years, LES results have proved to be predictive for non-reacting flows [2 – 6] and more recently also for reacting flows [7 – 12]. These results suggest that LES could be used in configurations as complex as aero and industrial gas-turbines for the prediction of mean reacting flows properties but also of flow instabilities. However, the CPU cost and the restitution time of LES in these configurations do not yet meet industrial requirements. Consequently, simpler tools must be developed so that their joint use with LES enables a deeper understanding of the physics, thus reducing the number of LES calculations. One such class of codes is Helmholtz solvers which are commonly found in many research centers and companies involved in thermacoustics research [1, 13 – 15]. These codes try to predict the frequencies and the structure of eigenmodes of the flow in the combustor assuming harmonic perturbations around a frozen mean state [1, 14]. Obviously, Helmholtz approaches require significant simplifications for the flow and cannot be expected to provide LES-like accuracy for the flow. However,

the acoustic analysis offered by Helmholtz methods is more complete than the LES results: Helmholtz solvers provide all possible modes frequencies and structure as well as their growth rates while LES will only evidence the modes which appear for one given regime. Moreover, doing parametric studies is impossible with LES: knowing for example which exhaust nozzle or which Helmholtz resonator can damp a given combustion instability is out of reach of LES but can be done with Helmholtz solvers.

Obviously, LES and Helmholtz codes are complementary methods to study combustion instabilities and more generally unsteady combustion. In this paper, the power of these combined tools is illustrated by considering a question which is the subject of multiple discussions in the combustion community: the existence and importance of rotating modes in swirling combustion [12, 16, 17]. It is well known that non-reacting swirling flows exhibit a variety of unstable modes [18 – 20]: the Precessing Vortex Core (PVC) is one of these modes (Fig. 1) for which the vortex axis destabilizes and spirals around the vortex initial direction. Such instabilities are observed for unconfined non-reacting flows [18] and also in the wakes of aircrafts [21 – 23] but also in confined combustion chambers where they often dominate the turbulent activity in the absence of combustion [12]. Because these instabilities appear so clearly for non-reacting flows, it is often assumed that they also dominate the reacting cases. For example, gas turbine burner flows are often tested with water to determine residence times and try to predict possible instabilities from the observation of the cold flow modes. Whether modes observed in such water channel experiments can be extrapolated to instabilities in the real combust-ing situation is an important question. Note that PVCs are hydrodynamic instabilities which usually do not couple with the acoustics of the chamber. In

reacting configurations, the acoustic generation due to the flame excites many modes of the chamber, sometimes leading to rotating modes which look like PVC but are actually due to the combination of transverse acoustic modes and not to a hydrodynamic instability. This paper describes such a situation in a swirled complex geometry combustor. The configuration is first presented. The LES and the Helmholtz solvers are then rapidly described. Cold flow results are discussed before presenting the computations for the reacting case.

## 2 Configuration

An important objective of this study is to present a methodology for the investigation of flame / acoustics interactions and combustion instabilities in realistic geometries. Therefore an industrial gas turbine burner (Fig. 2) mounted on a square laboratory combustion chamber in Karlsruhe [24] is considered. This burner is fed by two coaxial swirlers respectively called axial and diagonal swirler. The axial swirler, including its vanes, is fully computed in the LES, whereas the computational domain of the diagonal swirler begins at the trailing edge of the swirling vanes [12]. This burner is mounted on an combustion chamber with a square cross section (Fig. 3).

### 2.1 Meshes

The computational domain is the same for both solvers (LES and Helmholtz) but the number of mesh points can be drastically reduced for the computation of acoustic modes with the Helmholtz solver: indeed, the spatial resolution needed for LES is much higher than it is for the resolution of the first acous-

tic modes of the configuration in the Helmholtz computation. The grid for the reacting LES calculation contains 2,381,238 cells while the grid for the Helmholtz solver contains only 70,214 cells. Consequently, the computational cost of the Helmholtz solver is almost negligible compared to the LES. The computational time for the reacting LES is 280 CPU hours for one period of the high-frequency instability on a SGI O3800, whereas the computation of the first 13 acoustic modes with the Helmholtz code takes less than 10 CPU hours on the same machine.

## *2.2 Boundary conditions*

For such a study, boundary conditions must be well defined in terms of mean flow but also of acoustic impedances which must be the same in both computations (LES and Helmholtz). In this prospective study, purely reflecting boundary conditions are imposed at the inlets and outlet of the computational domain: the velocity profile is imposed at both axial and diagonal inlets (Fig.2) and the pressure is imposed at the outlet of the combustion chamber (Fig.3).

## **3 Numerical tools**

### *3.1 LES solver*

The solver used in this study ([www.cerfacs.fr/cfd/avbp.html](http://www.cerfacs.fr/cfd/avbp.html)) has already been validated and used in numerous studies for turbulent flows both non-reacting [4, 6, 25, 26] and reacting [12, 27 – 30]. A description of the parallel solver can

be found in [31] and its key features for this study are as follows. The code solves the compressible Navier-Stokes equations which allows to take into account acoustics. The Thickened Flame model for turbulent combustion [12, 28] enables the resolution of the flame front on typical LES meshes (whose characteristic cell size are usually much larger than flame thicknesses) while allowing ignition and extinction. This feature is of major interest in the computation of combustion instabilities since parts of the flame front can alternatively be quenched and re-ignited during the instability cycle. Accurate boundary conditions [29, 32] are mandatory for the prediction of unstable regimes since the acoustic impedances at the boundary drive the acoustic losses. Characteristic boundary conditions are used in the LES for all inlets, outlets and walls [31, 33]. The use of unstructured meshes enables the computation of complex geometries. The use of a high order numerical scheme [34] with minimal dispersion and dissipation is a key feature for the computation of turbulent flows, but also for the accurate resolution of the acoustic waves.

### 3.2 Helmholtz solver

If the reactive Navier Stokes equations are linearized around a mean state (index 0), the general form of the Helmholtz equation is obtained [1, 14]:

$$\nabla \cdot (c^2 \nabla p') - \frac{\partial^2}{\partial t^2} p' = -(\gamma - 1) \frac{\partial \dot{\omega}_T}{\partial t} - \gamma p_0 \nabla \vec{u} : \vec{u} \quad (1)$$

where  $p'$  is the pressure perturbation,  $\dot{\omega}_T$  is the unsteady local heat release,  $p_0$  is the average pressure and  $c$  is the local sound speed.  $c$  changes considerably in a reacting flow: it depends on the local value of  $\gamma$ , on the mean molecular weight  $W$  and on temperature:  $c = (\gamma RT/W)^{1/2}$  where  $R = 8.32 uSI$ . The

two forcing terms in the RHS of Eq. 1 are related to the outsteady combustion and turbulent noise respectively. To obtain this equation, the following assumptions are needed:

- Low Mach number flow
- No volume forces
- Linear acoustics (i.e. small perturbations)
- Large scale fluctuations.
- Homogeneous mean pressure.
- Constant polytropic coefficient  $\gamma$ .

The wave equation is usually not solved in the time domain but in the frequency domain by assuming harmonic pressure variations at frequency  $f = \omega/(2\pi)$  for pressure and for local heat release perturbations:

$$p' = \Re(P'(x, y, z) \exp(-i\omega t)) \quad (2)$$

$$\dot{\omega}_T = \Re(\Omega'_T(x, y, z) \exp(-i\omega t)) \quad (3)$$

with  $i^2 = -1$

Introducing Eq. (3) into Eq. (1) and neglecting the turbulent noise compared to the combustion forcing leads to the Helmholtz equation where the unknown quantities are the complex pressure oscillation amplitude  $P'$  at frequency  $f$  and the heat release amplitude field  $\Omega'_T$ :

$$\nabla \cdot (c^2 \nabla P') + \omega^2 P' = i\omega(\gamma - 1)\Omega'_T \quad (4)$$

This equation is the basis of three-dimensional Helmholtz codes. Knowing the sound speed ( $c$ ) distribution, *i.e.* knowing the local composition and temper-



ature, it provides the eigen frequencies  $\omega_k$  and the associated structure of the mode  $P'_k(x, y, z)$ . At this point, two approaches of increasing complexity are found :

- First, the effects of the unsteady combustion can be neglected by setting  $\Omega'_T = 0$ . This is equivalent to finding the eigenmodes of the burner, taking into account the presence of the flame through the mean temperature field but neglecting the flame effect as an acoustic active element.
- In a second step, the active effect of combustion can be taken into account if a model linking  $\Omega'_T$  and  $P'$  can be derived to close Eq. (4). This is usually the difficult part of the modeling because it requires the determination of the transfer function between acoustics and flame.

For the present study, the active effects of the flame were neglected ( $\Omega'_T = 0$ ) and a parallel iterative solver was used to solve Eq. 4 on hybrid meshes [35]. The required mean fields of sound speed is obtained by post-processing the LES results for the reacting flow so that the effect of the flame through the mean temperature field is properly accounted for. Details about solving Eq. 4 with general boundary conditions and acoustically active flame are discussed in [36, 37].

#### 4 Non-reacting flow: low-frequency rotating mode

For the non-reacting regime, pure air is injected in both axial and diagonal swirlers. The air is pre-heated to  $T_{cold} = 323$  K. The LES results have been successfully compared to experimental data in a previous paper [12] in terms of mean and *rms* values for both axial and tangential velocities. The agreement

between LES calculations and experimental results is good for the mean flow and the focus is set here on the analysis of unsteady phenomena and especially of turning modes.

To begin this analysis, the acoustic modes of the configuration, computed with the Helmholtz solver for the non-reacting regime are first listed in Tab. 1:

- Modes number 1 and 2 correspond respectively to the 1/4 wave (Fig. 4) and 3/4 wave (Fig. 5) longitudinal modes of the configuration.
- Modes number 3 and 4 (Fig. 6 and 7) are the two 1/2 wave transverse and 1/4 wave longitudinal modes of the combustion chamber: their frequencies are equal because the chamber has a square cross-section and the burner is axisymmetric.
- Mode number 5 (Fig. 8) is the 5/4 wave longitudinal mode.
- Modes number 6 and 7 (Fig. 9 and 10) are the two 1/2 wave transverse and 3/4 wave longitudinal modes of the configuration.

Considering now the LES results, the first obvious observation is that the instantaneous flow does not follow the symmetries of the geometry: since the burner axis is on axis of symmetry for the burner and the chamber, one would expect the radial components of the velocity ( $v$  and  $w$ ) to be zero on the burner axis, apart from turbulent fluctuations. However, plotting the third component of the velocity at point A *i.e.* on the burner axis (Fig. 3) shows that the symmetry is broken by a strong harmonic oscillation (Fig. 15 in [12]). The frequency of this oscillation is  $f_{cold} = 275$  Hz. This mode was also observed in the experiment at Karlsruhe University [24] at the frequency  $f_{exp} = 255$  Hz.

The frequency  $f_{cold}$  of the velocity oscillation on the burner axis does not match any of the frequencies listed in Tab. 1 showing that this oscillation is

not an acoustic mode. It is thus suggested that the unsteadiness is caused by a hydrodynamic mode, which can be characterized in terms of Strouhal number:  $St = fD/u_{bulk}$ , where  $f$  is the frequency of the instability,  $D$  the burner diameter and  $u_{bulk}$  the bulk velocity. For the present mode  $St = 0.62$ , which is typical of PVC in swirl flows [18 – 20]. Fig. 1 presents a generic PVC: the vortex due to the swirling motion, originally aligned with the burner axis breaks down at point S in a spiral form. This structure rotates, as a block, around the burner axis. The PVC can be tracked in the LES (Fig. 11) by the low pressure region near the vortex axis. In this configuration, the sense of winding of the spiral is opposite to that of the swirl (which is the same for axial and diagonal swirlers). However, the whole structure precesses in the same direction as the global rotation of the flow. In conclusion, the cold flow is dominated by a hydrodynamic mode (PVC) in which acoustics play no role.

## 5 Reacting flow: high frequency rotating mode

For the regime considered here, the diagonal swirler is fed with premixed methane/air while the axial swirler injects pure air. Both flows are pre-heated to 673 K and the global equivalence ratio is  $\phi = 0.5$ .

### 5.1 Analysis of LES results

The 275 Hz PVC evidenced in the cold flow is not present any more in the reacting regime which is considered here [12]. However, plotting  $w$  at point A, after the PVC has vanished (Fig. 12) shows that the symmetry of the flow is still broken by a strong harmonic oscillation. This oscillation dominates

the turbulent fluctuations and its frequency is determined through a FFT of the velocity signal on the burner axis (Fig. 13):  $f_{hot} = 1198$  Hz. Plotting the pressure field in a plane normal to the burner axis (Fig. 14) shows that this high frequency oscillation now corresponds to a rotating transverse mode: the points of minimum and maximum pressure are rotating around the burner axis at the frequency  $f_{hot}$ . Even though this mode is "turning" like the PVC observed without combustion, it is not hydrodynamically but acoustically controlled. Its frequency is not determined through a Strouhal scaling based on the burner dimension but through the acoustic eigenmodes of the chamber as shown in the next section.

### 5.2 Reconstruction of the rotating mode using acoustic eigenmodes

As for the cold flow, the list of the first eigen frequencies in the reacting regime are presented in Tab. 2. Though the frequencies are different (due to the increase in the temperature), the structure of these modes is exactly the same as for the cold flow (*c.f.* Sec. 4 and Fig. 4 to 10); and they are not repeated here.

Modes 3 and 4 are transverse modes sharing the same frequency, 1192 Hz, very close to that observed in the LES. It is possible to show that the rotating mode observed in the LES is actually the combination of these two modes (3 and 4). The pressure fluctuations induced by modes 3 and 4 can respectively be written:

$$p'_3(x, y, z, t) = A_3 \cos(\omega_3 t + \phi_3) F_3(x, y, z) \quad (5)$$

$$p'_4(x, y, z, t) = A_4 \cos(\omega_4 t + \phi_4) F_4(x, y, z) \quad (6)$$

where  $F_i$  is the mode shape,  $A_i$  the amplitude and  $\phi_i$  the phase for mode number  $i$ . Combining Eq. 5 and 6 with equal amplitudes ( $A_3 = A_4 = A$ ) but shifting mode 4 by 90 ( $\phi_3 = 0$ ;  $\phi_4 = -\pi/2$ ) leads to:

$$p'(x, y, z, t) = A(F_3(x, y, z) \cos(\omega_3 t) + F_4(x, y, z) \cos(\omega_4 t - \pi/2)) \quad (7)$$

As the mode shape is a direct output of the Helmholtz solver, the result of Eq. 7 can be reconstructed to generate the temporal evolution of the mode. This result is plotted in Fig. 15 and shows exactly the same structure as the rotating mode evidenced in the LES even though the pressure field obtained by LES displays slightly more complex patterns probably due to turbulence (Fig. 14). This proves that the high-frequency rotating mode evidenced in the LES of the reacting regime is the combination of the first two transverse acoustic modes of the combustion chamber, with equal amplitudes and a phase difference of  $\pi/2$ . Despite the fact that this result does not say why there transverse modes combine in this manner, it proves the acoustic nature of the turning mode for the reacting case.

### *5.3 Influence of the rotating mode on the flame shape*

The objective of this section is to show that in the LES, the shape of the flame is strongly affected by acoustic velocity fluctuations. The 1198 Hz mode is not simply forced by combustion. It also affects the flame itself leading to a self-sustained three-dimensional oscillation. These perturbations can be reconstructed from the Helmholtz solver results using the mass conservation

equation for the fluctuations:

$$\mathbf{u}' = \frac{\nabla p'}{i\rho\omega} \quad (8)$$

Combining Eq. 7 and Eq. 8 allows the reconstruction of the velocity perturbations corresponding to the acoustic rotating mode. Fig. 16 is a plot of axial-velocity fluctuations at the burner mouth generated by the rotating mode. At a given phase  $\phi = \omega t$  of the oscillation, the amplitude of the fluctuation is maximum at two locations close to the burner outer side and on opposite sides of the burner axis. At these two spots the axial velocity fluctuations have opposite signs. This pattern rotates around the burner axis at the frequency  $f_{hot} = 1198$  Hz.

The axial velocity fluctuations induced by the rotating acoustic mode occur at a critical location in the flow field: the burner mouth. Such fluctuations at a sudden expansion are known to generate vortex rings which can distort the flame front. This occurs in the present configuration: as shown in Fig. 19 the flame is distorted by a coherent structure in phase with the acoustic mode. The vortex is not toroidal as for vortex rings but has a spiral form which is the combination of two motions:

- (1) the rotating mode
- (2) and the convection by the mean flow field.

For a final quantitative validation of the structure of this mode, the phase of the axial velocity fluctuations from LES and Helmholtz solvers are now compared. Fig. 17 presents the pressure fluctuations at point  $C$  (Fig. 3) which is used as the phase reference to synchronize LES result with Eq. 7. Fig. 18 is the comparison of axial velocity fluctuations at point  $B$  (Fig. 3). The average ve-

locity is subtracted from the LES signal, and the fluctuations are normalized with a unique normalisation:

- The phases for the two solvers match exactly showing the power of the Helmholtz solver to predict acoustically induced velocity fluctuations.
- The fluctuations of  $u$  are strongly dominated by the acoustics showing that this flow is not dominated by turbulence but by acoustics.
- This result has implications for simulation: as this flow is obviously acoustically driven, the accurate computation of acoustic waves (low dispersion of numerical scheme, accurate boundary conditions) may be as critical as the modeling of the subgrid-scale turbulence.

## 6 Conclusion

Large-Eddy Simulations (LES) of an industrial-size burner mounted on an academic combustion chamber were conducted in both reacting and non-reacting regimes. The work focuses on the analysis of rotating modes evidenced in both LESs (cold and reacting). The joint use of a compressible LES solver and a Helmholtz solver enables the determination of the nature of these instabilities:

- For the cold flow the rotating mode is due to a hydrodynamic instability typical of swirling flows: Precessing Vortex Core (PVC). The Helmholtz solver shows that the frequency of this instability (275 Hz) does not correspond to an eigenmode of the configuration but can be predicted using a Strouhal scaling based on the bulk velocity and the burner mouth dimension.
- In the reacting regime, the flow still exhibits a rotating mode but at 1198

Hz. This mode is not hydrodynamic: it is acoustically controlled by a combination of the first two transverse modes of the combustor at 1192 Hz. The identification of the rotating mode as an acoustic mode is confirmed by the pressure fluctuation field: the complex structure of this mode evidenced in the LES can be successfully reconstructed from Helmholtz solver results.

This study suggests that a numerical prediction of turbulent combustion instabilities in a gas turbine requires:

- (1) A compressible LES solver: though the non-reacting part of this study could have been conducted with an incompressible solver, taking into account the acoustic waves is mandatory for the reacting case.
- (2) The joint use of two solvers (i.e. LES and Helmholtz). The Helmholtz solver explains the acoustic structure evidenced in the LES simulations by allowing the identification of all possible modes.

In the case of turning modes in swirled combustors, these two tools show that such modes can indeed be observed both for cold and reacting flows but that their nature is very different: for the cold flow, the rotating mode is an hydrodynamic mode but it becomes acoustically controlled when combustion is activated. Such an information is useful to understand the behavior of the combustor but also to help design which is often based on cold flow observation to study instabilities.

## **7 Acknowledgments**

This work has been supported by SIEMENS PG. The numerical simulations have been conducted on the computers of the French national computing cen-



ter CINES in Montpellier.

## References

- [1] Poinso, T. and Veynante, D., *Theoretical and numerical combustion*. R.T. Edwards, 2001.
  
- [2] Sagaut, P., *Large Eddy Simulation for incompressible flows*. Springer-Verlag, 2000.
  
- [3] Piomelli, U. and Chasnov, J. R., in *Turbulence and Transition Modelling* H. Hallbeck, D. S. Henningson, A. V. Johansson and P. H. Alfredsson, Kluwer Academic Publishers, 1996, p. 269 - 336.
  
- [4] Schlüter, J. and Schönfeld, T., *Flow Turb. and Combustion* 65: 177-203 (2000).
  
- [5] Mary, I. and Sagaut, P., *AIAA Journal* 40: 1139-1145 (2002).
  
- [6] Prière, C., Gicquel, L. Y. M., Kaufmann, A., Krebs, W. and Poinso, T., *J. of Turb.* 5: 1-30 (2004).
  
- [7] Janicka, J. and Sadiki, A., *Proc. of the Combustion Institute* 30: in press (2004).
  
- [8] Di Mare, F., Jones, W. P. and Menzies, K., *Combust. Flame* 137: 278-295

(2004).

[9] Huang, Y., Sung, H. G., Hsieh, S. Y. and Yang, V., *J. Prop. Power* 19: 782-794 (2003).

[10] Mahesh, K., Constantinescu, G. and Moin, P., *J. Comput. Phys.* 197: 215-240 (2004).

[11] Pierce, C. D. and Moin, P., *J. Fluid Mech.* 504: 73-97 (2004).

[12] Selle, L., Lartigue, G., Poinso, T., Koch, R., Schildmacher, K.-U., Krebs, W., Prade, B., Kaufmann, P. and Veynante, D., *Combust. Flame* 137: 489-505 (2004).

[13] Walz, G., Krebs, W., Hoffmann, S. and Judith, H., *Int. Gas Turbine & Aeroengine Congress & Exhibition*, p. (1999).

[14] Crighton, D. G., Dowling, A., Ffowcs Williams, J., Heckl, M. and Leppington, F., *Modern methods in analytical acoustics*. Springer Verlag, New-York, 1992.

[15] Zikikout, S., "Mécanisme d'instabilités de combustion dans un foyer à flammes non prémélangées," Doctorat, Université Paris-Sud Orsay, (1988).

[16] Evesque, S., Polifke, W. and Pankewitz, C., *9th AIAA / CEAS Aeroacoustics Conference and Exhibit*, p. AIAA-2003-3182 (2003).

- [17] Krebs, W., Flohr, P., Prade, B. and Hoffmann, S., *Combust. Sci. Tech.* 174: 99-128 (2002).
- [18] Billant, P., Chomaz, J.-M. and Huerre, P., *J. Fluid Mech.* 376: 183-219 (1998).
- [19] Lucca-Negro, O. and O'Doherty, T., *Prog. Energy Comb. Sci.* 27: 431-481 (2001).
- [20] Gupta, A. K., Lilley, D. G. and Syred, N., *Swirl flows*. Abacus Press, 1984.
- [21] Holzaepfel, F., *J. of Aircraft* 40: 323-331 (2003).
- [22] Holzaepfel, F., Hofbauer, T., Darracq, D., Moet, H., Garnier, F. and Ferreira Gago, C., *Aerospace Science and Technology* 7: 263-275 (2003).
- [23] Laporte, F. and Corjon, A., *Phys. Fluids* 12(5): 1016-1031 (2000).
- [24] Schildmacher, K.-U., Koch, R., Wittig, S., Krebs, W. and Hoffmann, S., *ASME TURBO EXPO 2000*, p. 2000-GT-0084 (2000).
- [25] Schlüter, J., Schönfeld, T., Poinsot, T., Krebs, W. and Hoffmann, S., *ASME TURBO EXPO 2001 Land, Sea and Air*, p. A. 2001-GT-0060 (2001).
- [26] Prière, C., Gicquel, T., Schönfeld, T., Poinsot, T., Kaufmann, P. and Krebs, W., *1st Int. Workshop on Trends in Numerical and Physical Modeling*

for *Turbulent Processes*, p. (2002).

[27] Angelberger, C., Egolfopoulos, F. and Veynante, D., *Flow Turb. and Combustion* 65: 205-22 (2000).

[28] Colin, O., Ducros, F., Veynante, D. and Poinso, T., *Phys. Fluids* 12: 1843-1863 (2000).

[29] Kaufmann, A., Nicoud, F. and Poinso, T., *Combust. Flame* 131: 371-385 (2002).

[30] Roux, S., Lartigue, G., Poinso, T., Meier, U. and Bérat, C., *Combust. Flame* in press: (2005).

[31] Moureau, V., Lartigue, G., Sommerer, Y., Angelberger, C., Colin, O. and Poinso, T., *J. Comput. Phys.* : 710-736 (2005).

[32] Ducruix, S. and Candel, S., *AIAA Journal* 42: 1550-1558 (2004).

[33] Poinso, T. and Lele, S., *J. Comput. Phys.* 101: 104-129 (1992).

[34] Colin, O. and Rudgyard, M., *J. Comput. Phys.* 162: 338-371 (2000).

[35] Lehoucq, R. and Sorensen, D., ([www.caam.rice.edu/software/ARPACK](http://www.caam.rice.edu/software/ARPACK)): (1997).

[36] Martin, C., Benoit, L., Nicoud, F. and Poinso, T., in *Proc of the Sum-*

mer Program Center for Turbulence Research, NASA Ames/Stanford Univ., Stanford, 2004, p. 377-394.

[37] Benoit, L. and Nicoud, F., *International Journal For Numerical Methods in Fluids*: (in press) (2005).

### List of Tables

1	List of eigen frequencies for the non-reacting case.	23
2	List of eigen-frequencies for the reacting case.	23

### List of Figures

1	Schematic representation of a generic PVC.	24
2	Burner.	25
3	Computational domain.	26
4	Mode number 1 is the 1/4 wave longitudinal acoustic mode ( $P'$ modulus).	27
5	Mode number 2 is the 3/4 wave longitudinal acoustic mode ( $P'$ modulus).	27

6	Mode number 3 is the 1/2 wave transverse in $y$ direction, 1/4 wave longitudinal acoustic mode ( $P'$ modulus).	28
7	Mode number 4 is the 1/2 wave transverse in $z$ direction, 1/4 wave longitudinal acoustic mode ( $P'$ modulus).	28
8	Mode number 5 is the 5/4 wave longitudinal acoustic mode ( $P'$ modulus).	29
9	Mode number 6 is the 1/2 wave transverse in $y$ direction, 3/4 wave longitudinal acoustic mode ( $P'$ modulus).	30
10	Mode number 7 is the 1/2 wave transverse in $z$ direction, 3/4 wave longitudinal acoustic mode ( $P'$ modulus).	30
11	Visualisation of the PVC in the LES by a pressure iso-surface.	31
12	Signal of $w$ at point A: the flow is dominated by a strong harmonic oscillation.	32
13	Spectrum of $w$ at point A: the dominant frequency is 1198 Hz (spectral resolution of 54 Hz).	32
14	Transverse structure of the high-frequency rotating mode in the reacting LES. Pressure minimum and maximum are rotating around the burner axis.	33
15	Transverse structure of the rotating mode reconstructed from the Helmholtz code results using Eq. 7.	34
16	Velocity fluctuations induced by the rotating mode at the burner outlet.	35

- 17 Normalised pressure fluctuations at point  $C$  in the LES (solid) and from the Helmholtz solver (dashed). 36
- 18 Normalised axial velocity fluctuations at point  $B$  in the LES (solid) and from the Helmholtz solver (dashed). 36
- 19 Distortion of the instantaneous flame front. Axial velocity fluctuations at the burner mouth, caused by the rotating acoustic mode, generate a helix shape vortex. 37

## Tables

---

Mode number	1	2	3	4	5	6	7
eigen frequency (Hz)	96.8	330.6	528.7	528.8	604.6	641.8	641.9

---

Table 1

List of eigen frequencies for the non-reacting case.

---

Mode number	1	2	3	4	5	6	7
eigen-frequency (Hz)	158.7	750.2	1192.2	1192.4	1349.6	1447.9	1448.1

---

Table 2

List of eigen-frequencies for the reacting case.



## Figures

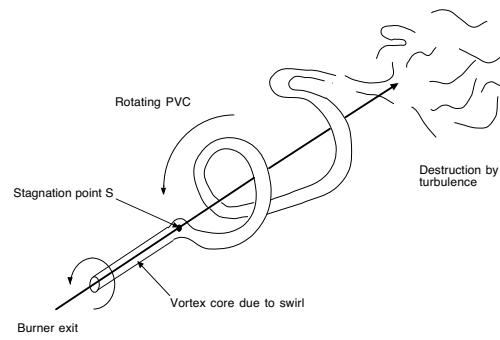


Fig. 1. Schematic representation of a generic PVC.

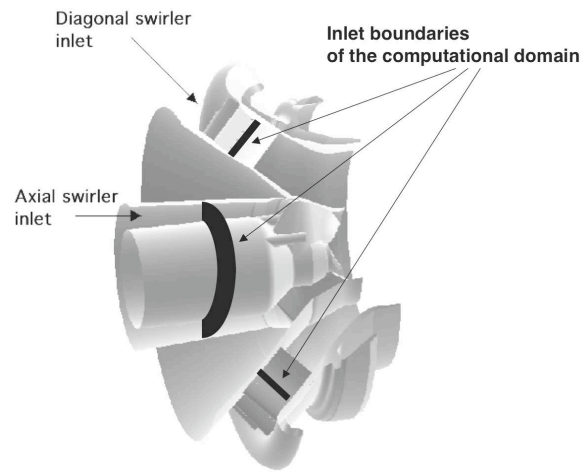


Fig. 2. Burner.

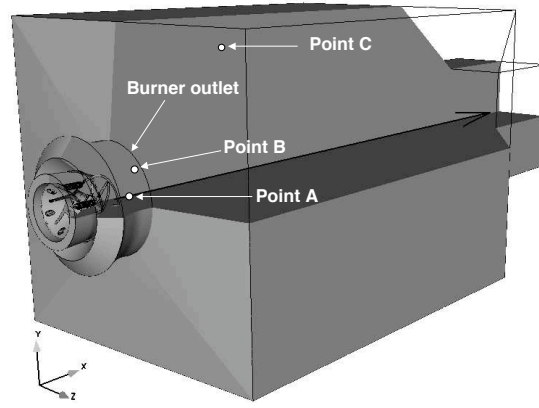


Fig. 3. Computational domain.

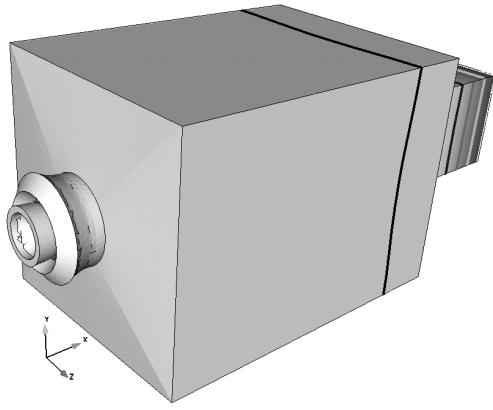


Fig. 4. Mode number 1 is the 1/4 wave longitudinal acoustic mode ( $P'$  modulus).

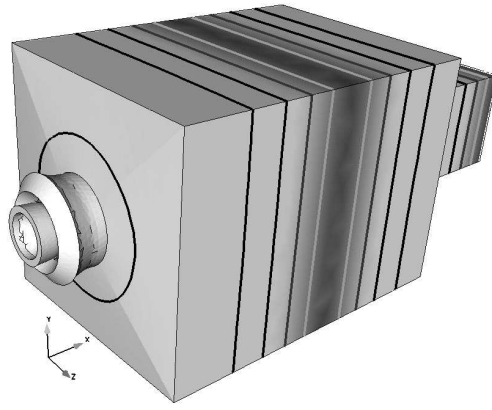


Fig. 5. Mode number 2 is the 3/4 wave longitudinal acoustic mode ( $P'$  modulus).

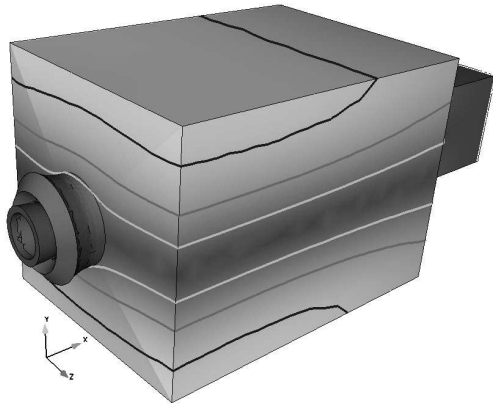


Fig. 6. Mode number 3 is the 1/2 wave transverse in  $y$  direction, 1/4 wave longitudinal acoustic mode ( $P'$  modulus).

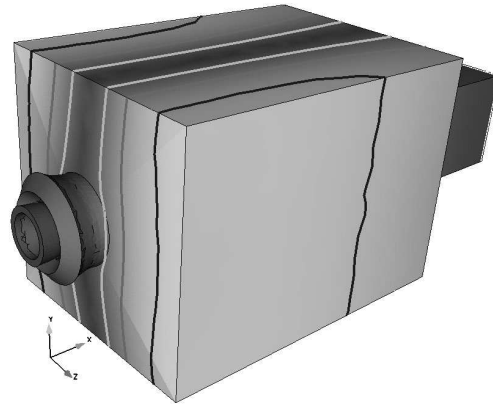


Fig. 7. Mode number 4 is the 1/2 wave transverse in  $z$  direction, 1/4 wave longitudinal acoustic mode ( $P'$  modulus).

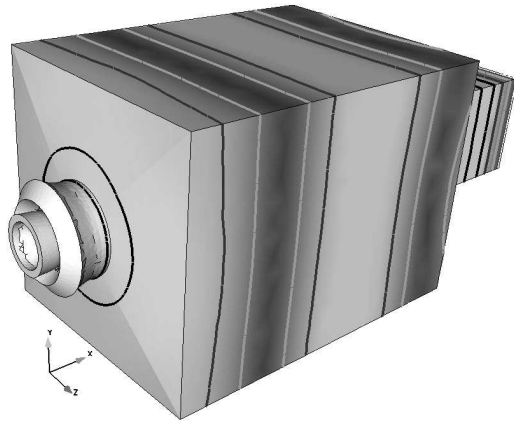


Fig. 8. Mode number 5 is the 5/4 wave longitudinal acoustic mode ( $P'$  modulus).

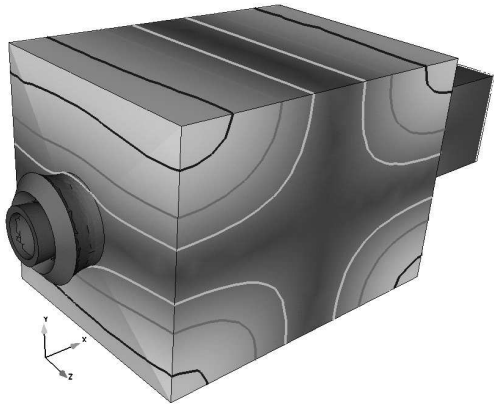


Fig. 9. Mode number 6 is the 1/2 wave transverse in  $y$  direction, 3/4 wave longitudinal acoustic mode ( $P'$  modulus).

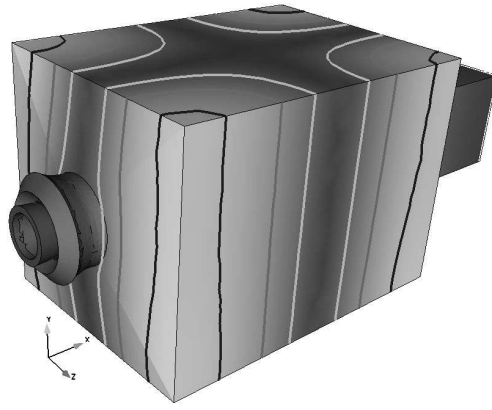


Fig. 10. Mode number 7 is the 1/2 wave transverse in  $z$  direction, 3/4 wave longitudinal acoustic mode ( $P'$  modulus).

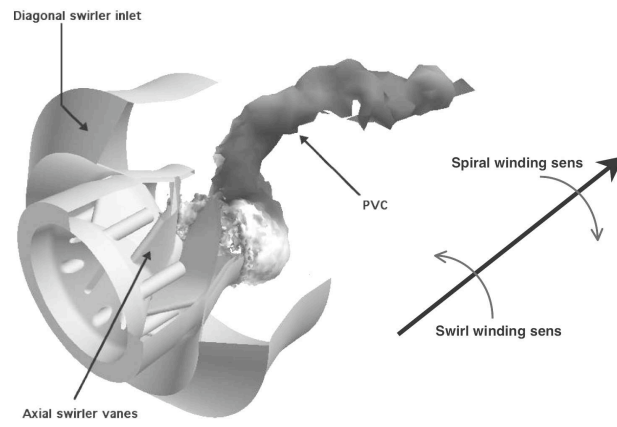


Fig. 11. Visualisation of the PVC in the LES by a pressure iso-surface.



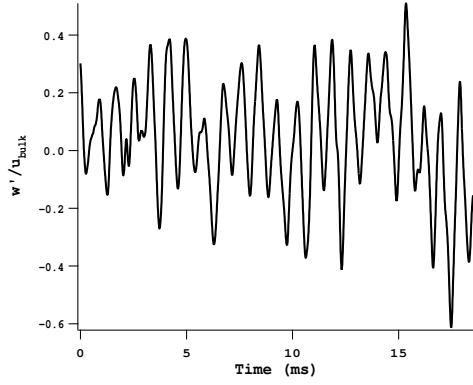


Fig. 12. Signal of  $w$  at point A: the flow is dominated by a strong harmonic oscillation.

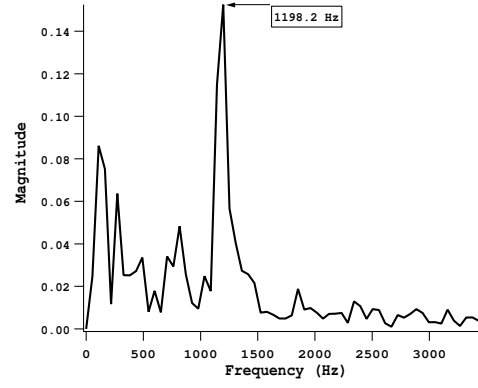


Fig. 13. Spectrum of  $w$  at point A: the dominant frequency is 1198 Hz (spectral resolution of 54 Hz).

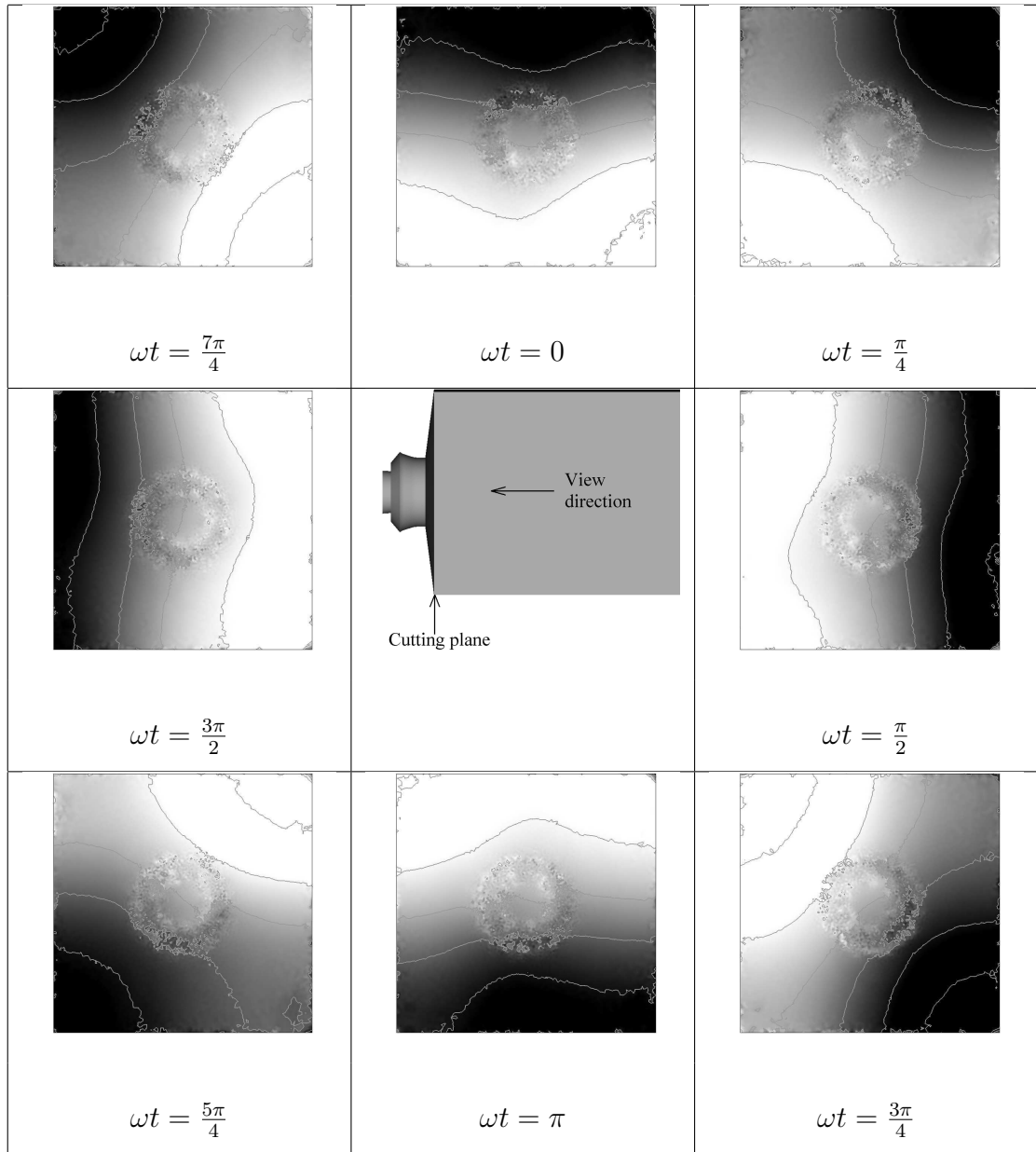


Fig. 14. Transverse structure of the high-frequency rotating mode in the reacting LES. Pressure minimum and maximum are rotating around the burner axis.

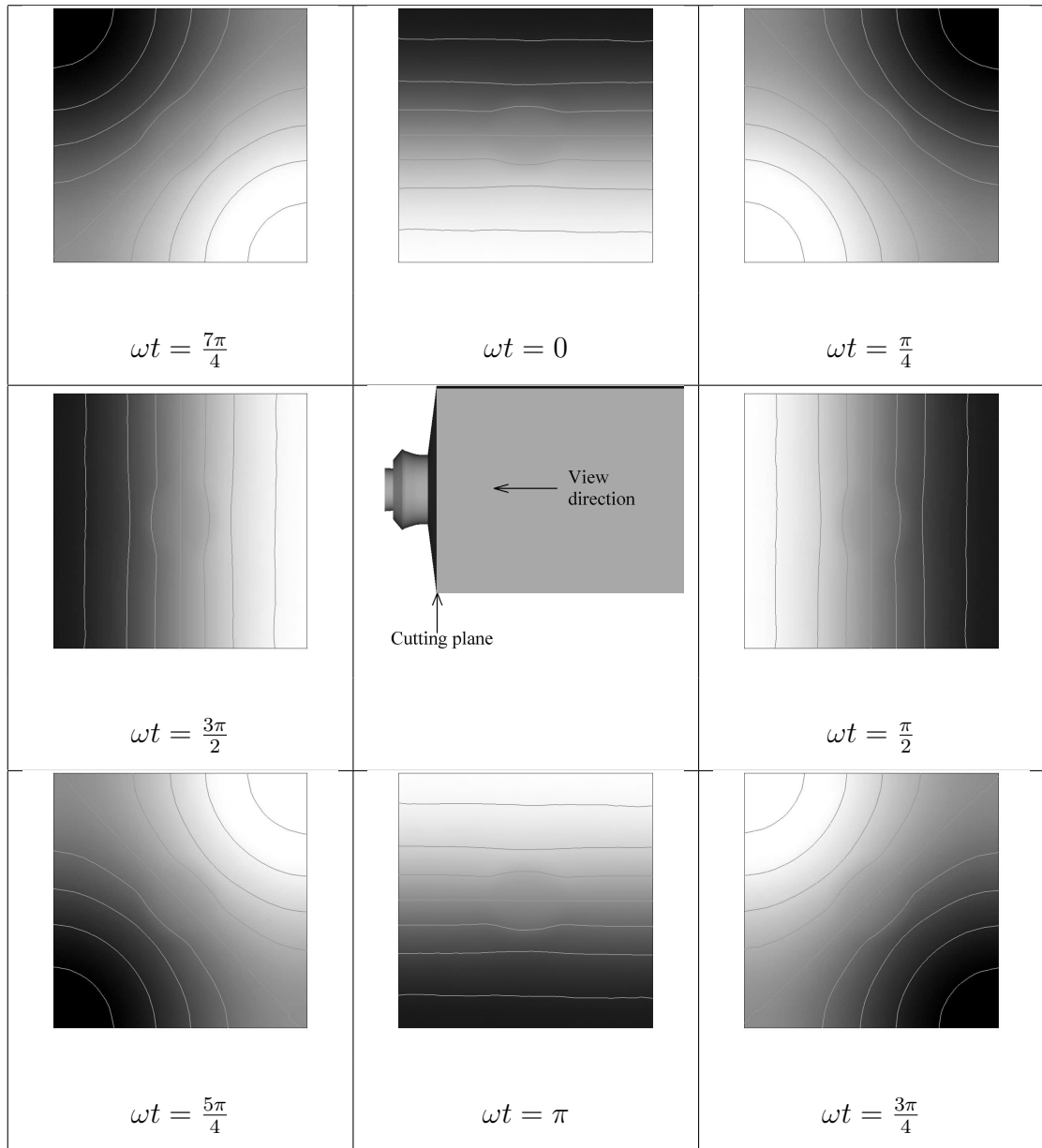


Fig. 15. Transverse structure of the rotating mode reconstructed from the Helmholtz code results using Eq. 7.

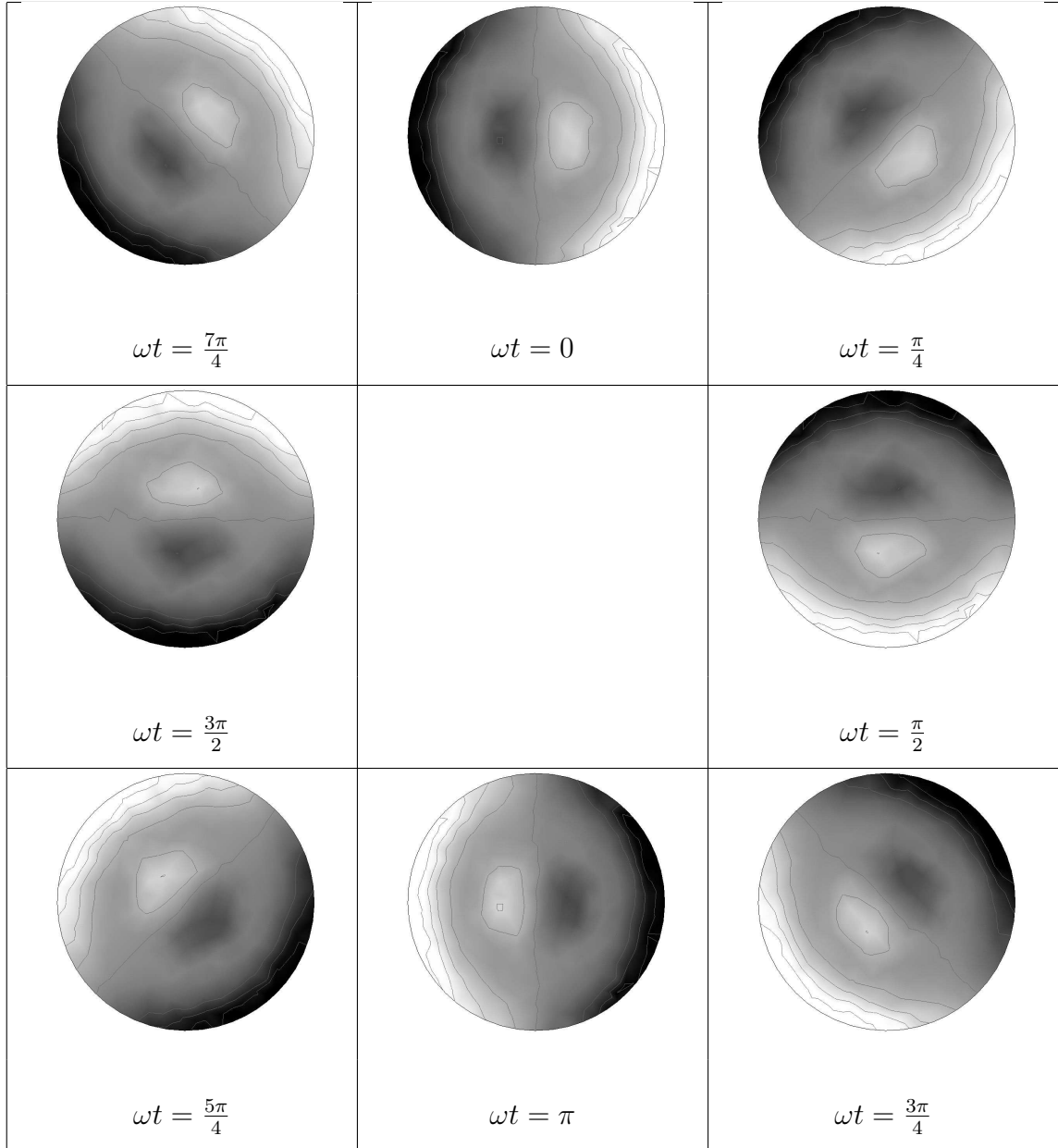


Fig. 16. Velocity fluctuations induced by the rotating mode at the burner outlet.

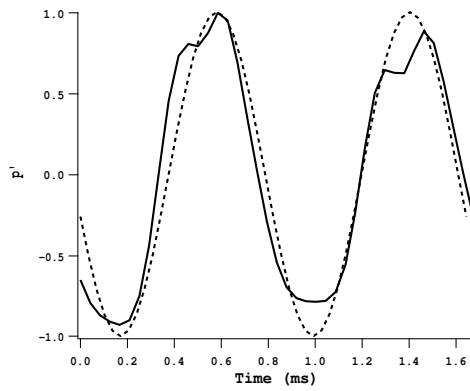


Fig. 17. Normalised pressure fluctuations at point  $C$  in the LES (solid) and from the Helmholtz solver (dashed).

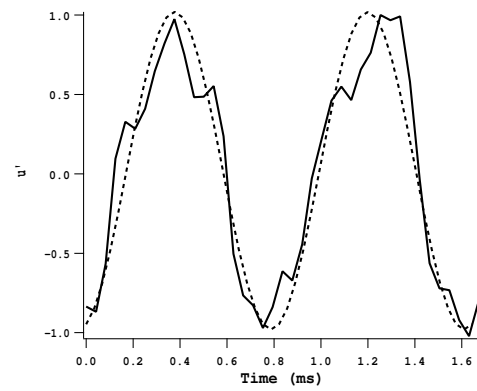


Fig. 18. Normalised axial velocity fluctuations at point  $B$  in the LES (solid) and from the Helmholtz solver (dashed).

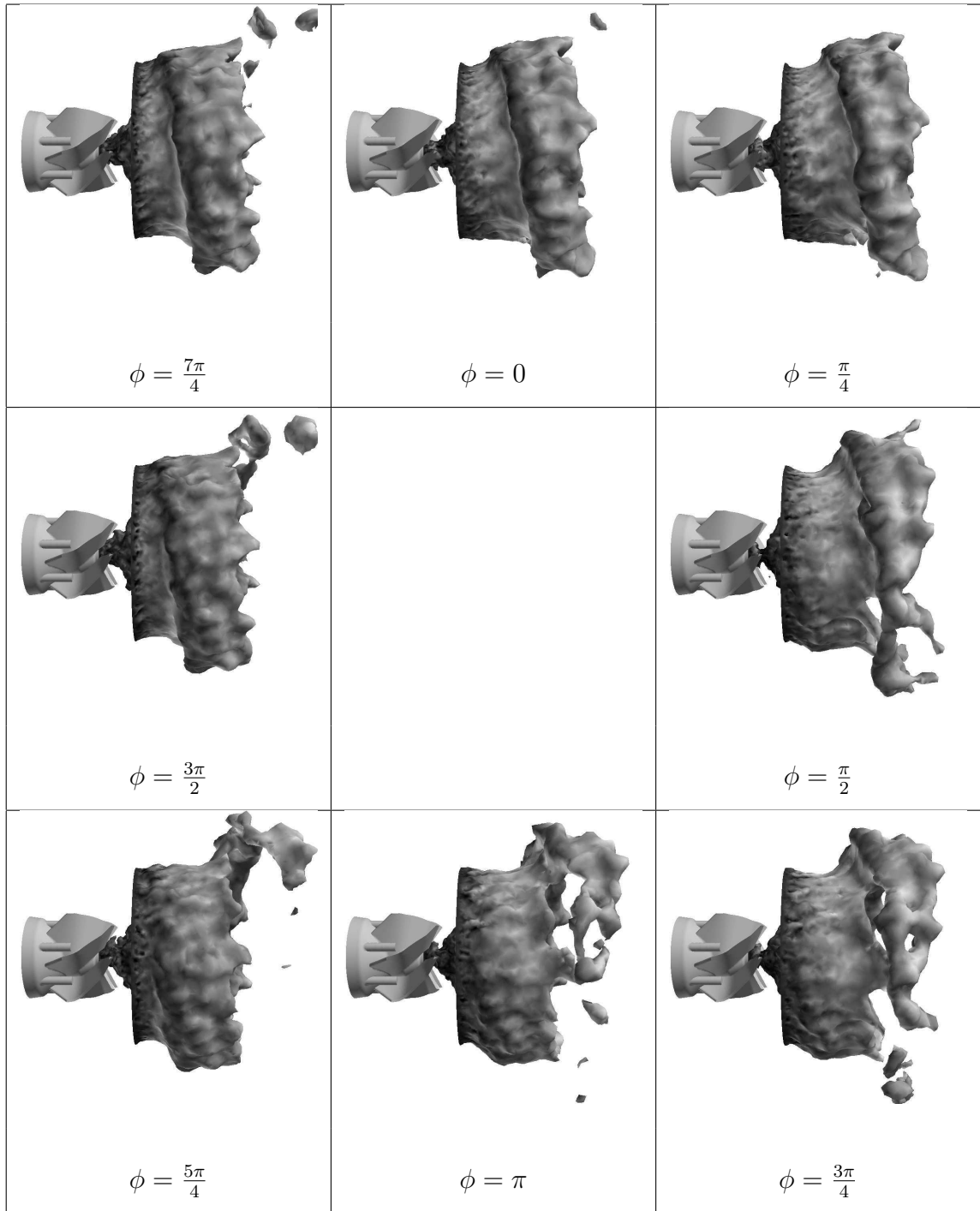


Fig. 19. Distortion of the instantaneous flame front. Axial velocity fluctuations at the burner mouth, caused by the rotating acoustic mode, generate a helix shape vortex.